Available online at www.sciencedirect.com

SciVerse ScienceDirect

Ceramics International 39 (2013) 1785–1792

CERAMICS INTERNATIONAL

www.elsevier.com/locate/ceramint

Dielectric properties of Ti substituted $Bi_{2-x}Ti_xO_{3+x/2}$ ceramics

Gourav Singla, K. Singh*

School of Physics and Materials Science, Thapar University, Patiala 147004, India

Received 26 June 2012; received in revised form 9 August 2012; accepted 9 August 2012
Available online 24 August 2012

Abstract

$(1-x)Bi_2O_3(x)TiO_2$ ($x=0.05$, 0.10, 0.15) materials were prepared by a conventional solid-state reaction technique. Dielectric properties of the materials were investigated using an LCR meter in the frequency range 20–10^6 Hz over the temperature range 100–500 °C. Both dielectric constant and loss tangent decreased with increasing Ti content in the present system. It was observed that dielectric relaxation peaks shift to a higher frequency with increasing temperature. Using the electric modulus equations, the relaxation process was evaluated and a parameter α ($0 \le \alpha < 1$) was extracted. Furthermore, the relaxation time as a function of temperature was calculated by an Arrhenius plot. A dielectric constant of ~54 was observed for sample $x=0.05$ due to its smaller grains and presence of higher defects.

© 2012 Elsevier Ltd and Techna Group S.r.l. All rights reserved.

Keywords: B. Grain boundaries; C. Dielectric properties; $B_{12}TiO_{20}$ phase; Relaxation

1. Introduction

High dielectric constant materials are required for various applications due to their electronic, photocatalytic and ferroelectric properties. In addition to the high dielectric constant, these materials should also have a good thermodynamic stability with low leakage current. Leakage current depends on the thickness of the materials. Presently, SiO_2 is being used as a high κ gate material. It has a high leakage current below certain thickness. Therefore, a lot of research is going on to search for high dielectric constant materials, with low leakage current and better mechanical properties. Oxides of Ti, Zr, Hf and Y are some of the materials having high dielectric constants [1]. However, all of them require high temperature sintering. On the other hand, doped bismuth oxide can be sintered at a low temperature with good dielectric properties because of its considerable high resistivity, permittivity and thermal stability up to 450 °C. Bismuth oxide (Bi_2O_3) has monoclinic crystal structure at room temperature, i.e., α-Bi_2O_3. This transforms to the cubic fluorite-type crystal structure δ-Bi_2O_3 above 725 °C with one-quarter of the available anion (oxygen) sites vacant [2–4]. It was reported that oxygen vacancies play a crucial role in relaxation and transport phenomena in this system. The diffusion of oxygen ions through oxygen vacancies is responsible for conduction in δ-Bi_2O_3 systems. The hopping of oxygen vacancy from one site to another has a close relationship with polarization conductivity, which is attributed to dielectric relaxation [5] since it has been observed that each migration of O^{2-} ions leads to dipole moment, which involves a dielectric relaxation process [6]. The doping of low valence cations such as Sr^{2+}, Ca^{2+}, and Ba^{2+} for Bi^{3+} enhances the ionic conductivity to create higher oxygen vacancies for maintaining charge balance in the system [7]. Dutta et al. [8] have investigated the dielectric properties of Ti doped CeO_2 systems. The maximum static dielectric constant is found to be ~30 in Ti doped CeO_2 systems. On the other hand, Yumamura et al. [9] have reported that Nd doping for CeO_2 is responsible in suppressing the interfacial polarization in this system. Contrary to this, the Zr doping in CeO_2 increases its dielectric constants. Kiran et al. reported the variation in dielectric constant 29–23 in $(Zn,Mg)TiO_3$ system depending on the processing conditions [10]. Lanfredi et al. reported that single crystals of $Bi_{12}TiO_{20}$ exhibited a high dielectric loss in the frequency range of 100–10^4 Hz [11].

*Corresponding author. Fax: +91 175 2393005.
E-mail address: kusingh@thapar.edu (K. Singh).

0272-8842/$ - see front matter © 2012 Elsevier Ltd and Techna Group S.r.l. All rights reserved.
http://dx.doi.org/10.1016/j.ceramint.2012.08.025

Frequency dependence of permittivity has also been reported in $(Bi_2O_2)_m-(TiO_2)_n$ compounds. Many researchers also reported interesting dielectric properties of different compounds such as $Bi_2Ti_2O_7$, $Bi_2Ti_3O_9$, $Bi_4Ti_3O_{12}$ and $Bi_{12}TiO_{20}$ [12–14]. In general, it is widely accepted that the oxygen vacancies in these systems play a very important role in deciding their dielectric properties.

Therefore, dielectric properties of the doped Bi_2O_3 systems will be very interesting and worth studying for different applications. In the present work, the effects of systematic Ti-doing for Bi in Bi_2O_2 systems on permittivity with respect to frequency and temperature are investigated. The obtained results are discussed in light of grain size, presence of secondary phase and oxygen vacancies changing with dopant concentration.

2. Experimental details

The oxides of Bi_2O_3 and TiO_2 were taken in appropriate stoichiometric amounts to prepare the composition of $(1-x)(Bi_2O_3)x(TiO_2)$ for $x=0.05$, 0.10, and 0.15 by using standard the solid-state reaction technique. The purity of the oxides was greater than 99.9%. Appropriate quantities of required constituent oxides of high-purity fine powders were thoroughly mixed in the presence of acetone for 2 h using a mortar and a pestle and dried in air. This mixture was heated at 700 °C for 4 h in air using a recrystallized alumina crucible and slowly cooled to room temperature. The calcined powder was ground and cold pressed after applying 13 kN/cm^2 pressure on pellets of 15 mm diameter and 2 mm thickness by adding poly(vinyl alcohol) as a binder. All the green pellets were sintered at 790 °C for 12 h in air followed by furnace cooling to avoid the volatization of Bi_2O_3. The density of the sintered samples was measured by Archimedes's method. Silver paste was used on both sides of pellets as electrodes to carry out dielectric measurement by the spring loaded two probe method in the temperature range of 100–500 °C. Dielectric response was measured using an Agilent 4284A analyzer which can cover a frequency range from 20 to 10^6 Hz. All the measurement is performed in air at the heating rate 5 °C/min with temperature stability ±1 °C. SEM was done on the fractured surface of the samples using a JEOL JSM-6510 LV equipment, respectively.

3. Results and discussion

3.1. Dielectric characterization

It has been confirmed by X-ray diffraction pattern that the $Bi_{2-x}Ti_xO_{3+x/2}$ system exhibits a single-phase $Bi_{12}TiO_{20}$ (BTO) in $x=0.15$. Contrary to this, samples with $x<0.15$ have a mixed phase viz BTO and monoclinic α-Bi_2O_3 as secondary phase. These results have been reported in our earlier report [15].

Fig. 1(a, b) shows the microstructure of $Bi_{2-x}Ti_xO_{3+x/2}$ ($x=0.10$ and $x=0.15$) sintered at 790 °C for 12 h. Sintered samples showed dense and uniform microstructure. Density of sintered samples obtained is more than 90% of the theoretical density. By comparing Fig. 1(a) and (b), it can be seen that at low doping concentration of Ti the second phase (Bi_2O_3) acts as a grain growth inhibitor and the grains look like spherulitic in nature as shown in Fig. 1(a). On the other hand, higher substitution of Ti leads to good grain growth with uniform and regular grains (Fig. 1(b)). Higher grain growth can be possible due to faster diffusion of Ti^{4+} ions as compared to Zr^{4+} ions [16]. Room temperature dielectric constant (ε') as a function of frequency (100–10^6 Hz) for $x=0.05$, 0.10 and 0.15 samples are shown in Fig. 2. It was observed that ε' shows frequency independent behavior above 10 kHz particularly, for the

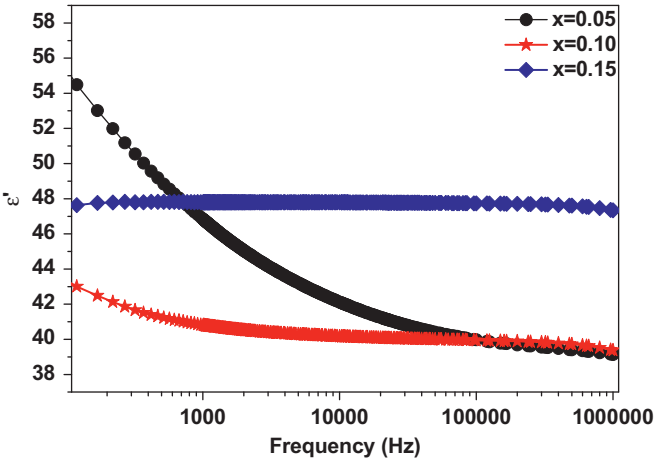

Fig. 2. ε' of $Bi_{2-x}Ti_xO_{3+x/2}$ with frequency at room temperature for different x.

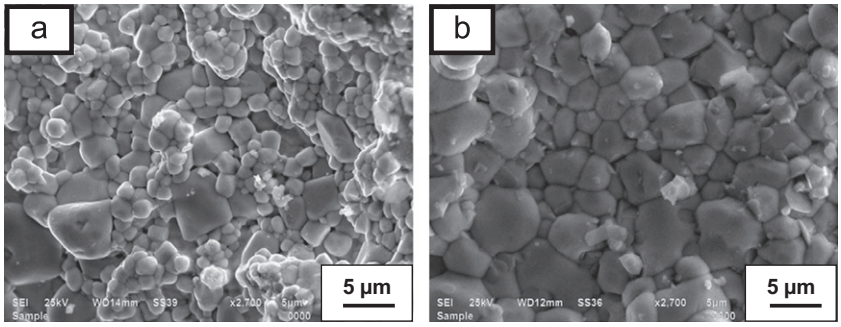

Fig. 1. Scanning electron micrographs of $Bi_{2-x}Ti_xO_{3+x/2}$. (a) $x=0.10$ and (b) $x=0.15$ samples.

$x=0.10$ sample. But frequency independent behavior for $x=0.05$ sample was observed above 100 kHz. Interestingly, the $x=0.15$ sample show frequency independent behavior throughout the testing frequency range as can be seen from Fig. 2. The highest dielectric constant is observed for $x=0.05$ sample. It may be ascribed due to lower grain size, higher oxygen vacancies and higher defects in this sample.

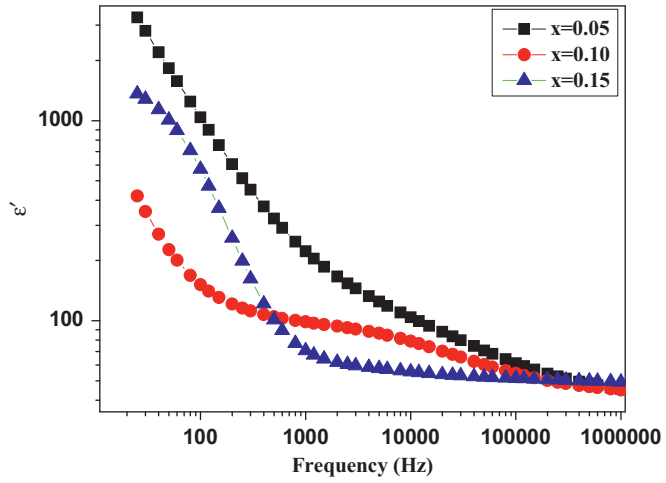

Fig. 3. ε' as a function of frequency for the $Bi_{2-x}Ti_xO_{3+x/2}$ system at 400 °C.

The frequency dependence of dielectrics constant (ε') at 400 °C is shown in Fig. 3 for $x=0.05$, 0.10 and 0.15 samples. From Fig. 3, it is clear that the frequency independent behavior of ε' shifts towards a higher-frequency range above $\sim 10^5$ Hz in all the samples. The ε' values of Ti doped sample in the low-frequency range were anomalously large and showed step-like behavior for all samples. The increment in dielectric constant with respect to frequency at a higher temperature (400 °C) is due to dominating interfacial polarization as compared to the orientation polarization. However, interfacial polarization is more pronounced in the $x=0.05$ sample.

The frequency dependences of real permittivity (ε') and dielectric loss (tan δ) of $Bi_{2-x}Ti_xO_{3+x/2}$ in a temperature range from 250 to 500 °C are shown in Fig. 4 for $x=0.10$ and $x=0.15$. It has been observed that Ti substitution for Bi reduced the dielectric constant. It is due to substitution of highly polarized bismuth ions with less polarized Ti^{4+} ions in the cation sub-lattice because Shirao et al. [17]

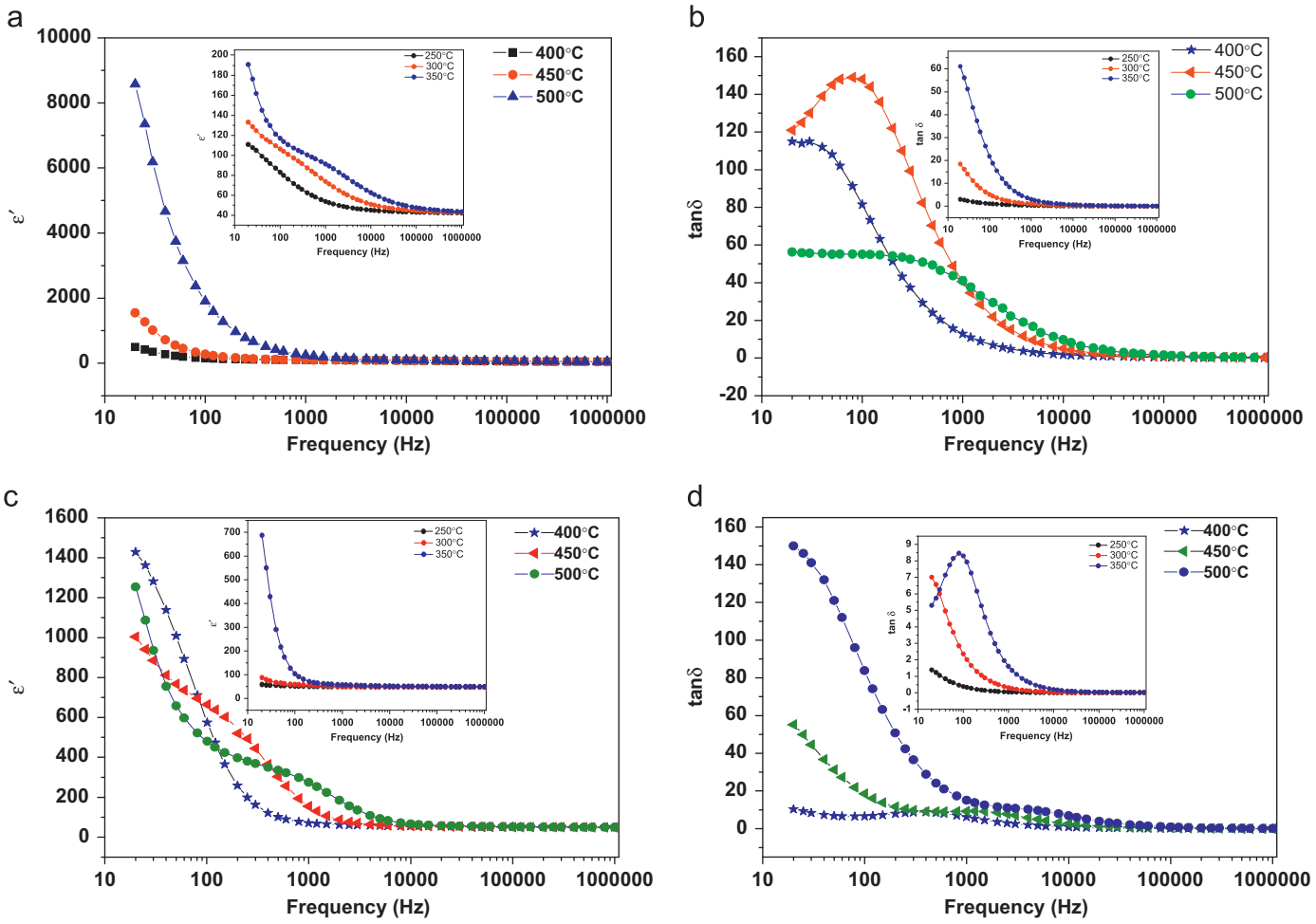

Fig. 4. Frequency dependent (a, c) real permittivity ε' and (b, d) tan δ of $Bi_{2-x}Ti_xO_{3+x/2}$ for $x=0.10$ and 0.15 respectively at different fixed temperatures.

observed that the polarization is proportional to the cube of ionic radius of the constituent's cation.

So, the dielectric constant of doped cubic bismuth oxide decreases with increasing concentration of less polarized Ti^{4+} cation, which is clear from the measured lower dielectric constant of the monophasic $x=0.15$ as compared to $x=0.10$ sample. It can be related to larger grain size of the $x=0.15$ sample. Similar results have been reported by Kiran et al. for the $(Zn,Mg)TiO_3$ system [10]. Additionally, the lower Ti substituted sample exhibits higher interfacial polarization as compared to the $x=0.15$ sample.

The decay of the dielectric constant becomes more diffuse and shifts to lower frequency range with decreasing temperature as given in the inset of Fig. 4. With increasing temperature, a high degree of dispersion of the permittivity curve is observed at lower frequency (<10 kHz), which is related to storage of several charge carriers (Bi_2O_3) at the grain boundaries, causing a conduction process or other defects [18,19]. This type of behavior has been reported in dielectrics [20]. There is an increase in magnitude of the dielectric constant observed with decreasing frequency at low frequencies. Sarkar and Nicholson [21] suggested that the large ε' values at lower frequencies were due to an electrolyte–electrode interfacial polarization process. At higher frequencies, dielectric constant decreases slowly and the maximum peak shifts to higher frequency as the temperature increases. Therefore, in a higher-frequency region dielectric constant follows non-Debye behavior ω^{n-1}. In the low-frequency region, the ions jump in the applied field direction and pile up at the high energy barrier sites. This results in increase of capacitance in the applied field direction. At high frequencies, the periodic reversal of the field takes place so rapidly that there are no excess ion jumps in the field direction. The capacitative effect disappears at high frequencies, which reduces the contribution of charge carriers to the dielectric constant. It can be seen that there is a decrease in ε' with increase in frequency. The imaginary parts of permittivity (ε'') as a function of frequency for $Bi_{2-x}Ti_xO_{3+x/2}$ ($x=0.05$, 0.10, 0.15) at temperature 500 °C are presented on a logarithmic scale in Fig. 5. The straight linear lines represent the theoretical fit based on the Johnscher-law [22] as follows:

$$\varepsilon''(\omega) = const. \times \omega^{n-1} \quad (1)$$

The magnitude of the exponent (n) can be considered to be very small, reflecting the level of non-ideality for the capacitance. So, the deviation of capacitance from the ideal behavior with increase in Ti^{4+} concentrations is a clear evidence of the existence of intrinsic defects [11,23].

The higher value of dielectric constant at lower frequency might be related to space charge polarization caused by impurities and crystal defects. In the present samples, the $x=0.05$ sample exhibits the highest dielectric constant due to the small grain size and higher number of grain boundaries (surface defects) as seen in Fig. 1(a, b). In our earlier reports, it has been observed, the presence of secondary phase impedes the grain growth; particularly

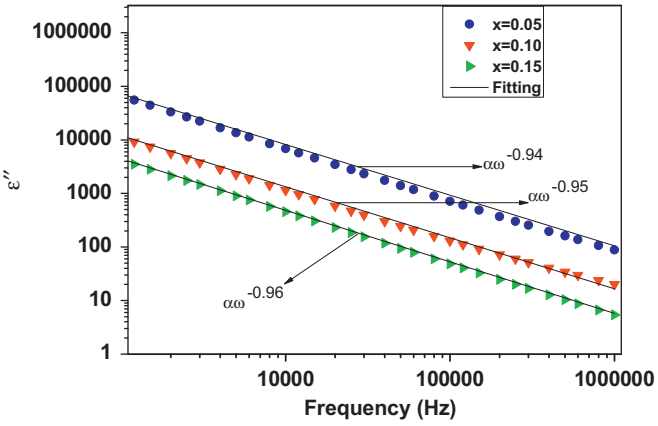

Fig. 5. Plots of universal dynamic response for $Bi_{2-x}Ti_xO_{3+x/2}$ ($x=0.05$, 0.10, 0.15) at temperature 500 °C.

$x=0.05$ and $x=0.10$ samples may lead to a higher dielectric constant as compared to the $x=0.15$ sample. So, the presence of secondary phase affects the dielectric constant by two ways. Firstly, the presence of secondary phase impedes the grain growth as seen in Fig. 1(a) and (b). Secondly, the presence of higher conducting secondary phase may lead to decrease in the dielectric constant (α-Bi_2O_3). Ultimately, it may be responsible for the higher dielectric losses in these samples.

The frequency dependences of dielectric loss $\tan\delta$ at different temperatures for $x=0.10$ and $x=0.15$ are shown in Fig. 4. At lower Ti concentration ($x<0.15$) $\tan\delta$ increases due to the segregation of secondary phase at the grain boundary, especially α-Bi_2O_3 which is known to be conducting in nature [24]. The $\tan\delta$ versus frequency curve exhibits a distinct relaxation peak in the low-frequency region. It is clearly evident from Fig. 4 that position of the dielectric loss peak shifts to higher frequencies as the temperature increases. This phenomenon is called thermal activated Debye-like relaxation. The relaxation process is determined by Debye-like relaxation time given by $\omega_{max}\tau = 1$, where ω_{max} is the maximum angular frequency. The continuous increment in tangent loss with decreasing frequency in the low-frequency region at lower temperatures (<350 °C) is a consequence of dominating ionic contribution [25] in $x=0.05$ and $x=0.10$ systems. This type of drop in $\tan\delta$ is not observed at a lower temperature. This means that the Debye-relaxation does not take place at a lower temperature [26].

The entire phenomenon as mentioned above is related to actuation of a hopping type mechanism, i.e., a small polaron hopping with a gradual decrease of electron–lattice coupling [27]. The effect of Ti- substitution on the dielectric behavior of the present samples can be clearly seen in terms of maxima shifting toward higher-frequency region, peak broadening and asymmetry in the peak. The shifting of maxima toward the higher-frequency region with increasing concentration of dopant indicates decrease in the relaxation time. As the concentration of Ti-substitution increases, the increase in the broadening and

asymmetry of the peaks suggests that there is an increase in the distribution of relaxation times [28]. According to the dielectric theory, the activation energy for dielectric relaxation could be calculated from the dielectric loss factor ε''. However, in the present oxide system, the loss factor (ε'') cannot give any idea of the dielectric relaxation process as also reported for many other oxide systems because it is attributed entirely to dc-conductivity which is usually dominant at high temperatures and low frequencies [29–33]. Therefore, the activation energy for the relaxation will be estimated by considering that the loss factor ε'' is proportional to tan δ [34].

The activation energy for relaxation can be calculated by the following Arrhenius equation:

$$\tau = \tau_0 \exp\left(\frac{E_a}{kT}\right) \quad (2)$$

where τ_0 is a pre-exponential factor, k is the Boltzmann constant, T is the temperature at which the relaxation peak has a maximum and E_a is activation energy required for the dielectric relaxation process. As shown in Fig. 6, the slope of the curve gives the activation energy. The activation energies (E_a) are 0.88 eV and 1.14 eV for $x=0.10$ and $x=0.15$, respectively. Higher E_a for $x=0.15$ is due to defect trapping influence, which can be associated to the strong affinity of the oxygen vacancies with small and less polarized Ti^{4+} ions. It implies that there is a decrease in mobile oxygen vacancies with increased concentration of TiO_2. In other words, it may be occurring due to ordering of oxygen vacancies as observed in many systems [15]. Additionally, it is also reported that Ti ions are more effective in trapping oxygen vacancies [35]. Clearly, the activation energy from relaxation conduction is nearly equal to that of our earlier study [15]. The difference in the activation energies obtained from the two different methods is due to the difficulty in distinguishing the bulk and grain boundary contribution of the samples [5].

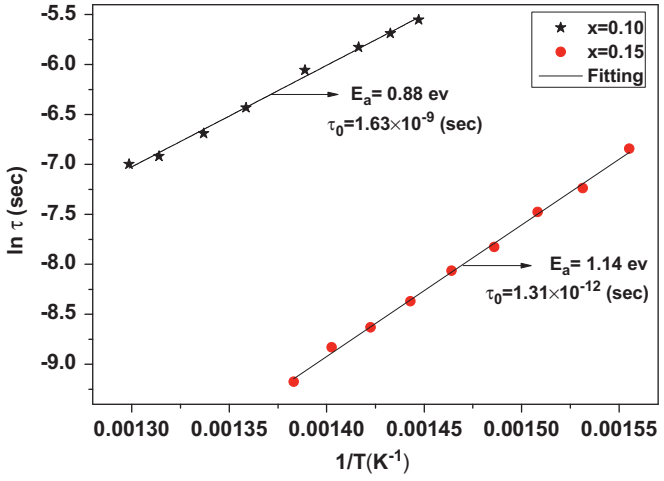

Fig. 6. Arrhenius relations $\ln \tau$ vs. $1/T$ for $Bi_{2-x}Ti_xO_{3+x/2}$ ($x=0.10$ and 0.15).

3.2. Temperature and frequency dependences of dielectric constant

Fig. 7 shows the temperature dependence of the dielectric constant of $Bi_{2-x}Ti_xO_{3+x/2}$ with various values of x. The dielectric constant decreases with increase in doping concentration of Ti. The value of the ε' initially remains constant as the temperature rises up to a particular point T_a. From the graph, it is also clear that the value of T_a increases with increase in Ti concentration. This may arise due to the presence of orientation and space charge polarization dominantly [36]. Additionally, T_a temperature decreases with increasing frequency for the same composition. This type of behavior might be attributed to low frequency as the dipoles are able to follow the applied field due to the slow process of orientation and space polarization as compared to ionic and electronic polarizations [37].

3.3. Electric modulus

Macedo et al. [38] introduced the electric modulus to study space charge relaxation phenomena. The effect of conductivity can be highly suppressed when all the data are presented in the form of electric modulus. Physically, the electric modulus corresponds to the relaxation of the electric field in the material when the electric displacement remains constant. Electric modulus represents the real dielectric relaxation process, which can be expressed as $M^* = 1/\varepsilon^*$. The value of M' and M'' can be evaluated by using the following relation:

$$M'(\omega) = \frac{\varepsilon'(\omega)}{\varepsilon'(\omega)^2 + \varepsilon''(\omega)^2} \quad \text{and} \quad M''(\omega) = \frac{\varepsilon''(\omega)}{\varepsilon'(\omega)^2 + \varepsilon''(\omega)^2} \quad (3)$$

The frequency dependences of M'' at various temperatures which are calculated using Eq. (3) are shown in Fig. 8. The relaxation peaks for $M''(\omega)$ shift to a higher-frequency region with increasing temperature. The shifting in peaks indicates the transition from a short range to long

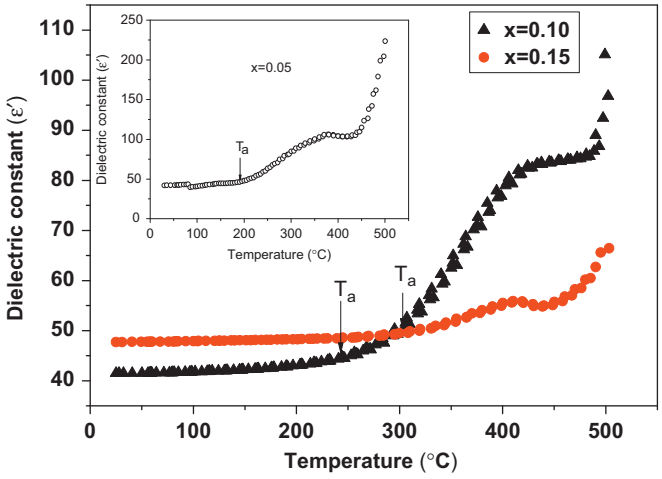

Fig. 7. ε' measured at 10 kHz for the composition $Bi_{2-x}Ti_xO_{3+x/2}$.

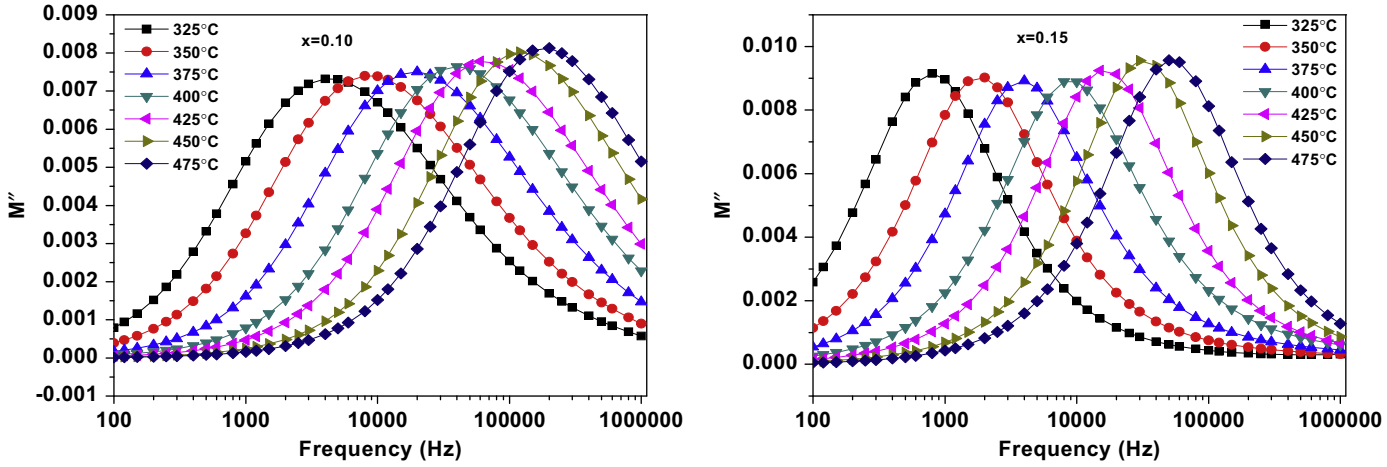

Fig. 8. Frequency dependence of M'' for $Bi_{2-x}Ti_xO_{3+x/2}$ ($x=0.10$ and 0.15) at various temperatures.

range mobility with decreasing frequency. It means that the relaxation rate for this process decreases with increasing temperature. The presence of peaks in the high-frequency region indicates that the ions are spatially confined to their potential wells and can execute only localized motion [39]. It has been observed that the height of the modulus peak increases with increase in Ti concentration in the present sample. This may be correlated with low capacitance value in the $x=0.15$ sample. This result is in good agreement with the data given in Fig. 5. The most probable conductivity relaxation time τ is calculated from the peak frequency f_{max} using the relation: $2\pi f_{max}\tau = 1$.

It is observed that they closely follow the Arrhenius law

$$\tau_M = \tau_{0M} \exp\left(\frac{E_{aM}}{kT}\right) \tag{4}$$

Based on the high-temperature data, the activation energies for conduction processes are 0.99 eV and 1.1 eV with $\tau_{0,M} \approx 10^{-13}$ s for $x=0.10$ and $x=0.15$, respectively. This data clearly indicates that Ti doping increases the activation energy of the dielectric relaxation. In contrast to this, it decreases the conduction process.

It is interesting to note that the activation energy obtained from $\tan\delta$ curves represents the localized conduction (dielectric relaxation) whereas the activation energy obtained from M'' represents nonlocalized conduction (long range conduction). Interestingly, the activation energies obtained from the two different methods are almost the same, which indicates that the chemical natures of conduction species are the same [40]. Moreover, it is clear from the calculation that the activation energies of the localized and nonlocalized conduction decrease with increase in Ti concentration in the Bi_2O_3 system.

It is well known that many dielectric relaxation processes can be described by the modified Debye model, i.e., the Cole–Cole's equation as follows:

$$\varepsilon = \varepsilon_\infty + \frac{(\varepsilon_s - \varepsilon_\infty)}{[1+(i\omega\tau)^{(1-\alpha)}]} \tag{5}$$

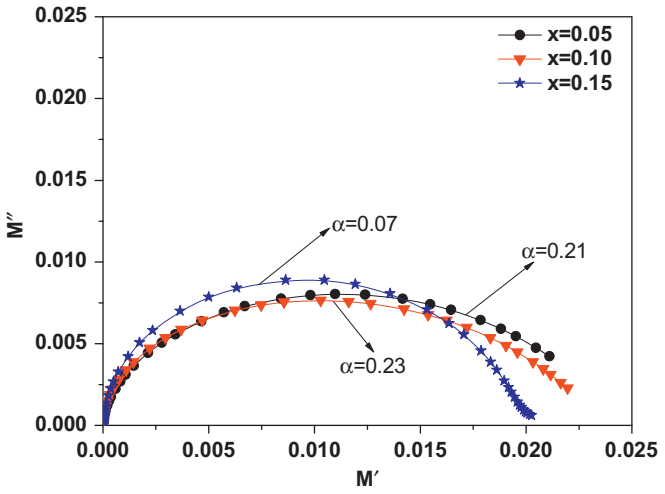

Fig. 9. Cole–Cole plot of complex electric modulus of $Bi_{2-x}Ti_xO_{3+x/2}$ at 400 °C.

where ε_0 is the static permittivity, ε_∞ is the permittivity at high frequency, ω is the angular frequency, τ is the mean relaxation time, and α is the angle of the semicircle arc or dispersion angle. The data fit according to Eq. (5), by which the parameter α calculated is shown in Fig. 9. The value of α represents the deviation from an ideal Debye model. Additionally, it also gives an idea of the interaction between the dipoles. The obtained value of α for the sample $x=0.15$ is very close to zero which suggests a behavior close to that of the state of a single relaxation time for the dipoles. This factor α is also well known to be related with the interaction of charge carriers during the conduction processes. In this way, this should be higher when several charges accumulate at the grain boundaries [18]. In the current systems, the amount of conducting Bi_2O_3 phase decreases along the grain boundary, which is why the value of α is lower at higher value of x. So, it is clearly indicated that high concentration of Ti leads to ideal Debye model conditions. Obviously, $x=0.15$ system

in single phase materials are responsible for this type of behavior.

4. Conclusion

The dielectric constant at room temperature is higher in the $x=0.05$ sample due to higher defects and smaller grain size. On the other hand, the $x=0.10$ sample shows the lowest dielectric constant among all the present samples. The dielectric constant decreases with increasing temperature in the $x=0.15$ sample. But the dielectric constant increases with the increase in temperature for $x=0.10$ and $x=0.05$ samples. It indicates that $x=0.15$ is predominantly governed by the orientation polarization phenomenon. High Ti substitution for Bi sample leads to the ideal Debye model. At room temperature, the ε' is frequency independent, particularly in the $x=0.15$ sample. This sample can be used for wide frequency based applications.

Acknowledgments

Authors are very grateful to the Defence Research and Development Organization (DRDO), New Delhi, India, for providing the financial grant under vide Letter no. ERIP/ER/1103976/M/01/1411 and Mr. Ravi Shukla for valuable suggestions.

References

[1] G.D. Wilk, R.M. Wallace, J.M. Anthony, High-κ gate dielectrics: current status and materials properties considerations, Journal of Applied Physics 89 (2001) 5243–5275.
[2] H.A. Harwig, On the structure of bismuth sesquioxide: the α, β, γ, and δ phases, Zeitschrift fuer Anorganische und Allgemeine Chemie 444 (1978) 151–166.
[3] A. Helfen, S. Merkourakis, G. Wang, M.G. Walls, E. Roy, K. Yu-Zhang, Y. Leprince-Wang, Structure and stability studies of electrodeposited δ-Bi_2O_3, Solid State Ionics 176 (2005) 629–633.
[4] H.A. Harwig, A.G. Gerards, Electrical properties of the α, β, γ, and δ phases of bismuth sesquioxide, Journal of Solid State Chemistry 26 (1978) 265–274.
[5] K.P. Padmasree, R.A. Montalvo-Lozano, S.M. Montemayor, A.F. Fuentes, Electrical conduction and dielectric relaxation process in $Ce_{0.8}Y_{0.2}O_{1.9}$ electrolyte system, Journal of Alloys and Compounds 509 (2011) 8584–8589.
[6] R. Gerhardt, Impedance and dielectric spectroscopy revisited: distinguishing localized relaxation from long-range conductivity, Journal of Physics and Chemistry of Solids 55 (1994) 1491–1506.
[7] E.P. Kharitonova, V.I. Voronkova, V.K. Yanovskii, Electrical conductivity of Bi_2WO_6 crystals doped with Ca^{2+}, Pb^{2+}, Sr^{2+}, and Ba^{2+}, Inorganic Materials 41 (7) (2005) 757–759.
[8] G. Dutta, S.K. Saha, U.V. Waghmare, Effects of Zr and Ti doping on the dielectric response of CeO_2: a comparative first-principles study, Solid State Communications 150 (2010) 2020–2022.
[9] H. Yamamura, S. Takeda, K. Kakinuma, Dielectric relaxations in the $Ce_{1-x}Nd_xO_{2-\delta}$ system, Solid State Ionics 178 (2007) 1059–1064.
[10] S.R. Kiran, G. Sreenivasulu, V.R.K. Murthy, V. Subramanian, B.S. Murty, Effect of grain size on the microwave dielectric characteristics of high-energy ball-milled zinc magnesium titanate ceramics, Journal of the American Ceramic Society (2012) 1–7.
[11] S. Lanfredi, J.F. Carvalho, A.C. Hernandes, Electric and dielectric properties of $Bi_{12}TiO_{20}$ single crystals, Journal of Applied Physics 88 (1) (2000) 283–287.
[12] S.P. Yordanov, I.S. Ivanov, C.P. Carapanov, Dielectric properties of the ferroelectric $Bi_2Ti_2O_7$ ceramics, Journal of Physics D: Applied Physics 31 (1998) 800–806.
[13] S.P. Yordanov, C.P. Carapanov, I.S. Ivanov, P.T. Cholakov, Dielectric properties of the ferroelectric $Bi_2Ti_3O_9$ ceramics, Ferroelectrics 209 (1998) 541–552.
[14] H.S. Shulman, D. Damjamovic, N. Setter, Niobium doping and dielectric anomalies in bismuth titanate, Journal of the American Ceramic Society 83 (3) (2000) 528–532.
[15] G. Singla, P.K. Jha, J.K. Gill, K. Singh, Structural, thermal and electrical properties of Ti^{4+} substituted Bi_2O_3 solid systems, Ceramics International 38 (2012) 2065–2070.
[16] J. Zhai, X. Yao, J. Shen, L. Zang, H. Chen, Structural and dielectric properties of $Ba(Zr_xTi_{1-x})O_3$ thin films prepared by the sol–gel process, Journal of Physics D: Applied Physics 37 (2004) 748–752.
[17] K. Shirao, T. Iiada, K. Kazuko, Y. Iwadate, Refractive indexes and electronic polarizabilities of molten $HoCl_3$–NaCl and $HoCl_3$–KCl mixtures, Journal of Alloys and Compounds 281 (1998) 163–168.
[18] J.C. M'Peko, J. Portelles, F. Calderon, G. Rodriguez, Dielectric anomaly and low frequency dispersion in ferroelectric materials at high temperatures, Journal of Materials Science 33 (1998) 1633–1637.
[19] F.I.H. Rhouma, A. Dhahri, J. Dhahri, M.A. Valente, Applied Physics A (2012)http://dx.doi.org/10.1007/s00339-012-6935-1.
[20] A.K. Jonscher, A new understanding of the dielectric relaxation of solids, Journal of Materials Science 16 (1981) 2037–2060.
[21] P. Sarkar, P.S. Nicholson, Electric field relaxation studies in the CeO_2–Y_2O_3 system, Journal of Physical Chemistry of Solids 50 (1989) 197–206.
[22] A.K. Jonscher, The universal dielectric response, Nature (London) 267 (1977) 673–679.
[23] K.V. Rao, A. Smakula, Dielectric properties of cobalt oxide, nickel oxide, and their mixed crystals, Journal of Applied Physics 36 (1965) 2031–2038.
[24] H.T. Martirena, J.C. Burfoot, Grain-size and pressure effects on the dielectric and piezoelectric properties of hot-pressed PZT-5, Ferroelectrics 7 (1974) 151–152.
[25] Md.G. Masud, B.K. Chaudhuri, H.D. Yang, High dielectric permittivity and room temperature magneto-dielectric response of charge disproportionate $La_{0.5}Ba_{0.5}FeO_3$ perovskite, Journal of Physics D: Applied Physics 44 (255403) (2011) 1–8.
[26] S. Rachna, S. Bhattacharyya, Surya M. Gupta, Dielectric properties and ac-conductivity analysis of $Bi_{3.25}La_{0.75}Ti_3O_{12}$ ceramic using impedance spectroscopy, Journal of Physics and Chemistry of Solids 69 (2008) 822–829.
[27] M.A.L. Nobre, S. Lanfredi, Ferroelectric state analysis in grain boundary of $Na_{0.85}Li_{0.15}NbO_3$ ceramic, Journal of Applied Physics 93 (2003) 5557–5562.
[28] Dillip K. Pradhan, R.N.P. Choudhary, C. Rinaldi, R.S. Katiyar, Effect of Mn substitution on electrical and magnetic properties of $Bi_{0.9}La_{0.1}FeO_3$, Journal of Applied Physics 106 (024102) (2009) 1–10.
[29] E. Iguchi, S. Nakayama, F. Munakata, M. Kurumada, Y. Fujie, Ionic conduction due to oxygen diffusion in $La_{0.8}Sr_{0.2}GaO_{3-\delta}$ electrolyte, Journal of Applied Physics 93 (2003) 3662–3664.
[30] E. Iguchi, N. Kubota, T. Nakamori, N. Yamamoto, K.J. Lee, Polaronic conduction in n-type $BaTiO_3$ doped with La_2O_3 or Gd_2O_3, Physical Review B 43 (1991) 8646–8649.
[31] E. Iguchi, K. Ueda, W.H. Jung, Conduction in $LaCoO_3$ by small-polaron hopping below room temperature, Physical Review B 54 (1996) 17431–17437.
[32] E. Iguchi, Y. Tokuda, H. Nakatsugawa, F. Munakata, Electrical transport properties in $LiMn_2O_4$, $Li_{0.95}Mn_2O_4$, and $LiMn_{1.95}B_{0.05}O_4$ (B=Al or Ga) around room temperature, Journal of Applied Physics 91 (2002) 2149–2154.
[33] N. Sangwong, W. Somphan, P. Thongbai, T. Yamwong, S. Meansiri, Applied Physics A (2012)http://dx.doi.org/10.1007/s00339-012-6897-3.

[34] M. Kurumada, H. Hara, E. Iguchi, Oxygen vacancies contributing to intragranular electrical conduction of yttria-stabilized zirconia (YSZ) ceramics, Acta Materialia 53 (2005) 4839–4846.
[35] A. Kaiser, A.J. Feighery, D.P. Fagg, J.T.S. Irvine, Electrical characterization of highly titania doped YSZ, Ionics 4 (1998) 215–219.
[36] H.T. Fan, S.S. Pan, X.M. Teng, C. Ye, G.H. Li, L.D. Zhang, δ-Bi_2O_3 thin films prepared by reactive sputtering: fabrication and characterization, Thin Solid Films 513 (2006) 142–147.
[37] C.Y. Chung, Y.S. Chang, G.J. Chen, C.C. Chung, T.W. Huang, Effects of bismuth doping on the dielectric properties of $Ba(Fe_{0.5}Nb_{0.5})O_3$ ceramic, Solid State Communications 145 (2008) 212–217.
[38] P.B. Macedo, C.T. Moynihan, R. Bose, The role of ionic diffusion in polarization in vitreous ionic conductors, Physics and Chemistry of Glasses 13 (1972) 171–179.
[39] J.S. Kim, Electric modulus spectroscopy of lithium tetraborate ($Li_2B_4O_7$) single crystal, Journal of the Physical Society of Japan 70 (2001) 3129–3133.
[40] O. Raymonda, R. Font, N. Suárez-Almodovar, J. Portelles, J.M. Siqueiros, Frequency–temperature response of ferroelectromagnetic $Pb(Fe_{1/2}Nb_{1/2})O_3$ ceramics obtained by different precursors. Part II: impedance spectroscopy characterization, Journal of Applied Physics 97 (084108) (2005) 1–8.